



Shape fidelity and sterility assessment of 3D printed polycaprolactone and hydroxyapatite scaffolds

Franca Scocozza^{1,2} · Mirena Sakaj³ · Ferdinando Auricchio¹ · Stefania Marconi¹ · Pietro Riello³ · Cinzia Ferrari^{4,5} · Laura Cansolino⁴ · Laura Catenacci⁶ · Milena Sorrenti⁶ · Marco Scatto^{3,7} · Michele Conti¹

Received: 20 November 2020 / Accepted: 13 July 2021
© The Author(s) 2021

Abstract

Polycaprolactone (PCL) and hydroxyapatite (HA) composite are widely used in tissue engineering (TE). They are fit to being processed with three-dimensional (3D) printing technique to create scaffolds with verifiable porosity. The current challenge is to guarantee the reliability and reproducibility of 3D printed scaffolds and to create sterile scaffolds which can be used for in vitro cell cultures. In this context it is important for successful cell culture, to have a protocol in order to evaluate the sterility of the printed scaffolds. We proposed a systematic approach to sterilise 90%PCL-10%HA pellets using a 3D bioprinter before starting the printing process. We evaluated the printability of PCL-HA composite and the shape fidelity of scaffolds printed with and without sterilised pellets varying infill pattern, and the sterility of 3D printed scaffolds following the method established by the United States Pharmacopoeia. Finally, the thermal analyses supported by the Fourier Transform Infrared Spectroscopy were useful to verify the stability of the sterilisation process in the PCL solid state with and without HA. The results show that the use of the 3D printer, according to the proposed protocol, allows to obtain sterile 3D PCL-HA scaffolds suitable for TE applications such as bone or cartilage repair.

Keywords Polycaprolactone · Hydroxyapatite · 3D printing · Bone tissue engineering · Sterility · Shape fidelity

Franca Scocozza and Mirena Sakaj equally contributed in this work.

✉ Michele Conti
michele.conti@unipv.it

- ¹ Dept. of Civil Engineering and Architecture, University of Pavia, Pavia, PV, Italy
- ² Dept. of Electrical, Computer and Biomedical Engineering, University of Pavia, Pavia, PV, Italy
- ³ Dept. of Science and Technology of Bio and Nanomaterials, University of Ca' Foscari, Venice, VE, Italy
- ⁴ Dept. of Clinical Surgical Sciences, University of Pavia, Pavia, PV, Italy
- ⁵ Animal Welfare and Radiobiology Service Centre, University of Pavia, Pavia, PV, Italy
- ⁶ Dept. of Drug Science, University of Pavia, Pavia, PV, Italy
- ⁷ Nadir S.R.L. C/O Scientific, Campus University of Ca' Foscari, Venice, VE, Italy

Introduction

The choice of biomaterial and fabrication method are two critical factors for the adoption of scaffolds in tissue engineering (TE) and regenerative medicine, which use scaffolds to promote cell growth and new tissue formation.

Currently, biocompatible synthetic thermoplastic polymers, e.g., polycaprolactone (PCL), polypropylene fumarate (PPF), polylactic acid (PLA), polyglycolic acid (PGA) and their copolymers have been used in TE [1]. These materials have well-fit mechanical properties, so they are used to make scaffolds for bone and cartilage TE. PCL is widely used thanks to hydrolysis and enzymatic digestion for a tunable period of time up to 2 years, which is the time span for bone healing [2]. Unfortunately, PCL has poor hydrophilicity, and it lacks bioactivity; this issue can be partially solved by incorporate bioactive agent, e.g., hydroxyapatite (HA), the main compound of the inorganic phase of bone, which allows PCL to enhance its mechanical properties, cell adhesion, and proliferation to better mimic bone tissue properties and promote regeneration process [3, 4]. For example, Kim et al. [5] produced composite scaffolds with various

HA contents (0%, 10%, 15%, and 20% wt.) for bone TE applications. They observed that all the PCL-HA composite scaffolds could greatly help the bone tissue regeneration. The increase of HA content increases mechanical properties and *in vitro* apatite-forming ability. According to Tian and colleagues [6], scaffolds surface morphology has changed because of the addition of HA particles the polymer: PCL-HA scaffolds surface roughness is much higher compared to PCL scaffolds, promoting the adhesion and proliferation of several different cell types better compared to a smooth surface [7, 8]. Moreover, the thermoplastic feature and PCL ability to be mixed with some additives by melt compounding technology make it fit to be processed with a wide variety of additive manufacturing (AM) techniques [9], referred to as three-dimensional (3D) printing (3DP), able to create verifiable and reproducible porous scaffolds [10]. There are indeed several research studies which propose 3D printed PCL-HA based scaffolds for TE applications [11, 12]. It is in this context that the current challenge is to guarantee the reliability, predictability, and reproducibility of 3D printed scaffolds and, at the same time, the evaluation of their sterility degree [13–15]. These two aspects can affect each other, therefore it is important to consider them together, to guarantee the effectiveness of the printing process. Unfortunately, these aspects are dealt separately in literature.

Generally, the effects of HA inclusion in the 3D printed PCL-based scaffolds are quantitatively assessed using the Differential Scanning Calorimeter (DSC), the Scanning Electron Microscope (SEM), the infrared spectroscopy, the mechanical test, and the cell adhesion and the proliferation test [16]. Trachtenberg and colleagues [17] generated biologically relevant scaffolds for *in vitro* and *in vivo* bone TE applications. They investigated the effect of the surfactant on scaffold properties, including printing solution viscosity, fiber diameter, porosity, pore size, interconnectivity, and compressive mechanical properties. Gerdes et al. [18] quantified the effect of process variables, namely pressure, temperature, and linear print speed on the dimension and shape fidelity of the extruded strands. These assessments were made using *in situ* optical imaging and analysis. Park and colleagues [19] made porous interconnected scaffolds with good mechanical properties using PCL, and PCL/HA blend scaffold with a shifted pattern for TE. They assessed scaffold porosity by means of micro-computed tomography, moreover they performed X-ray diffraction and Fourier transform infrared (FT-IR) analysis, mechanical and *in vitro* biological test.

However, the discussed papers did not consider the sterilisation issue that is an important element for TE applications. In fact, it is necessary to create sterile scaffolds which can be used for *in vitro* *in vitro* cultures and *in vivo* cell applications. If it doesn't, the possibility of contamination is very high, jeopardizing the result of cell culture. In this

context, thermoplastic materials, such as PCL, are used but they can hardly be sterilised with standard techniques (e.g., autoclave) due to the low melting temperature (60 °C). Furthermore, the starting raw material (pellets and/or powders) is often not produced in sterile conditions, therefore it is possible that contamination occurs. In this context, the current challenge is to evaluate sterility degree of 3D printed scaffolds [20–22].

Bugno and colleagues [23] have extensively faced the sterilisation issue. The authors evaluated the microbial detection efficiency of the BacT/Alert® system for the detection of aerobic and anaerobic microorganisms and they compared it with the pharmacopoeia sterility testing.

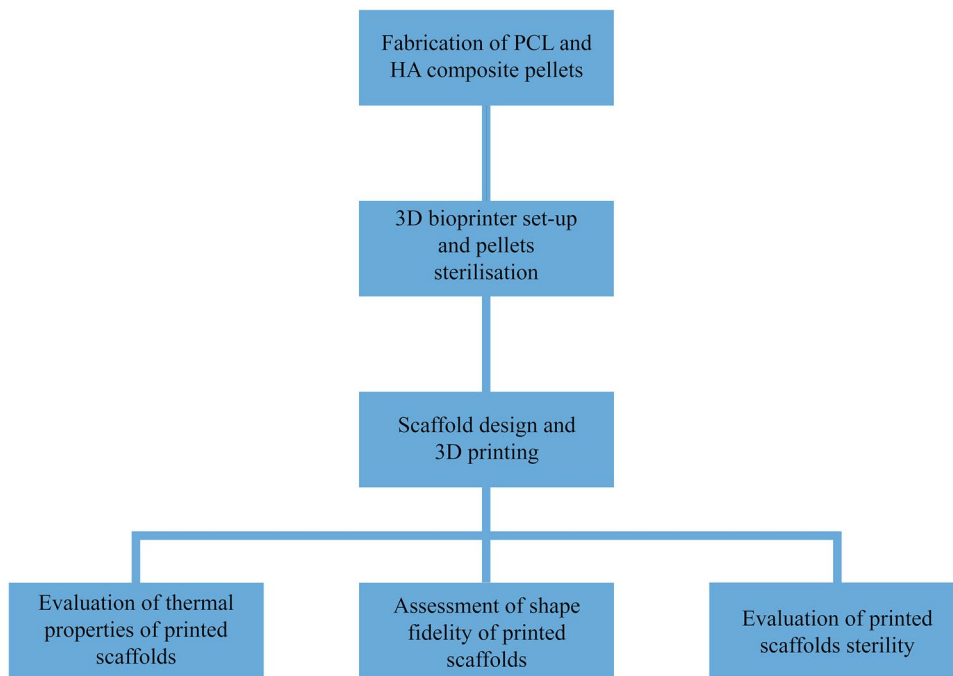
The polymeric contamination from a wide variety of microorganisms is a critical limitation for the use of polymeric materials for biomedical applications. It is important to choose an appropriate sterilisation technique to effectively sterilise biodegradable scaffolds but at the same time to keep structural and biochemical integrity. According to Dai et al. [24], most standard sterilisation techniques used in the clinical settings, e.g., ethylene oxide, autoclave, and gamma ray, have been used to sterilise biodegradable scaffolds, but these attempts have been largely unsuccessful. This is because biodegradable scaffolds are more sensitive to the conditions required by standard sterilisation methods. There are few contributions on the antibacterial properties of PCL-HA scaffolds for bone TE [25].

In light of these considerations, the goal of the present study is to carry out a feedstock to create a 3D printable composite of PCL blended with 10 HA% wt. which has sterility features, hence useful in TE applications. To achieve this, we proposed a systematic approach to sterilise 90%PCL-10%HA pellets using a 3D bioprinter before starting the printing process. We assessed the printing performance of PCL-HA scaffolds using the proposed sterilisation process, comparing the results with a standard approach. Afterwards we investigated the sterility degree of 3D printed scaffolds following the method established by the United States Pharmacopoeia (USP) [26]. Moreover, thermoplastic properties of 3D printed scaffolds were assessed to verify if the sterilisation process affected the thermal properties of the material.

Experimental

The proposed protocol involves the following steps (Fig. 1): i) fabrication of PCL and HA composite pellets fit for 3D printing, ii) 3D bioprinter set-up and pellets sterilisation, iii) scaffolds design and 3D printing, iv) evaluation of the 3D printed scaffolds thermal properties, v) assessment of printing performance, vi) evaluation of scaffolds sterility

Fig. 1 Summary of paper workflow

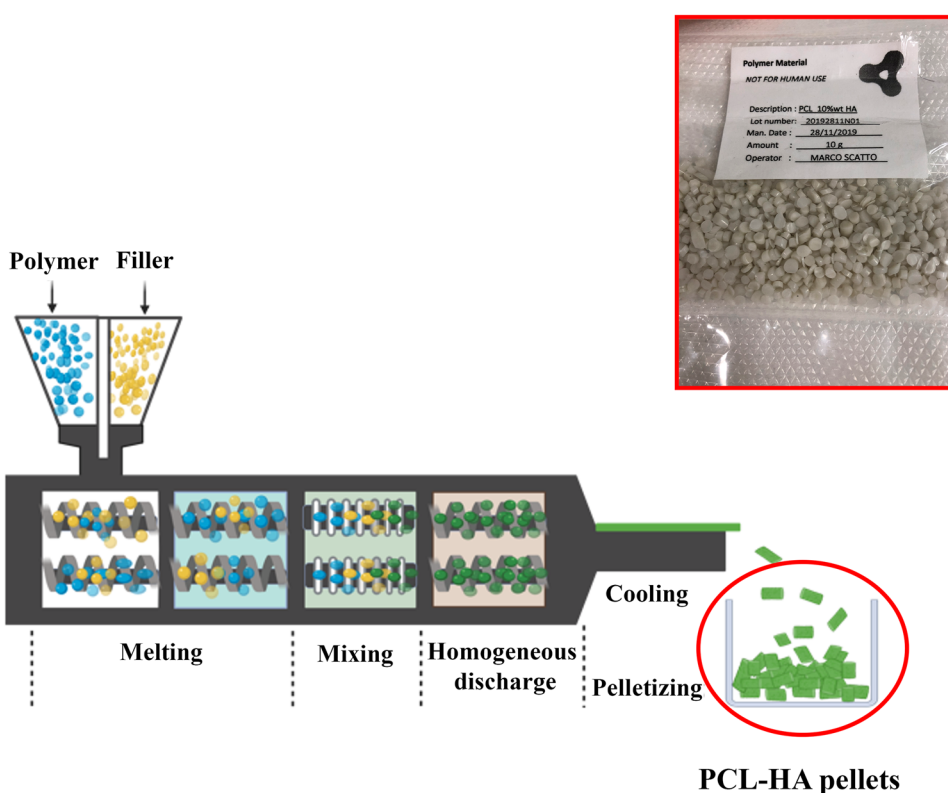


Fabrication of PCL and HA composite pellets

The 90% PCL and 10% HA composite has been produced by Nadir s.r.l. (Italy, www.nadir-tech.com), here in after referred to as 90%PCL-10%HA. The

production of 90%PCL-10%HA composite was carried out with a laboratory scale Co-rotating Twin Screw Extruder (Fig. 2) installed at Nadir s.r.l. Laboratory c/o University of Cà Foscari (Venice), endowed with a 11 mm diameter screw and a length-to-diameter ratio of 40. The screw profile

Fig. 2 Representation of laboratory scale Co-rotating Twin Screw Extruder installed at Nadir s.r.l. laboratory used for fabricating 90%PCL-10%HA composite pellets. PCL pellets (polymer) were fed into the main hopper with a volumetric feeder, then HA powder (filler) was fed with a second volumetric feeder thanks to a double inlet. composite wire was taken at the exit of the mold, solidified in the air and pelletized



is divided into eight zones with three interposed kneading sections. PCL pellets were fed into the main hopper with a volumetric feeder, while HA powder was fed with a second volumetric feeder thanks to a double inlet. The screw rotation speed and barrel temperature were fixed at 80 rpm and 60 °C respectively for the first zone and 65 °C for the following zones. The 90%PCL-10%HA wire was taken at the exit of the extruder. To avoid bacterial contamination, the composite wire was solidified in the air (rather than water) and was subsequently pelletized in a pelletizing machine.

3D bioprinter set-up and pellet sterilisation

3D bioprinter

The 90%PCL-10%HA pellets were 3D printed using Cellink INKREDIBLE+ (Cellink AB, Sweden), shown in Fig. 3a, a pneumatic extrusion-based 3D bioprinter with dual heated printheads (max 130 °C) and UV LED curing system (365 nm and 405 nm). INKREDIBLE+ is equipped with a patented Clean Chamber Technology that allows it to be used directly on the laboratory bench. The HEPA 13 filter and positive air pressure use ensure a sterile environment during the printing process. The process starts from a 3D virtual geometry that is translated into machine instructions by means of a slicing software, which generates the coordinates of the printing head in each layer along with appropriate instructions to control the material extrusion. The printing head positioning system has a 10 microns resolution in the three axes. For the 3D printing the 90%PCL-10%HA composite we used an aluminum cartridge and a 0.5 mm

metal nozzle which is able to withstand temperatures above 50 °C (Fig. 3b).

Sterilisation protocol of the 3D bioprinter and pellets

We used a 3D bioprinter to sterilise the printing area and the 90%PCL-10%HA pellets to produce sterile products. In the first place, a Petri dish glass was placed on a print-bed, then an aluminum cartridge was connected to a nozzle and it was filled with 90%PCL-10%HA pellets. Finally, the cartridge was inserted into the printhead and kept at 120 °C for 30 min. Meanwhile, the 365 nm wavelength UV led was switched-on to sterilise the printing area. Once the sterilisation process was completed, the temperature was decreased to 90 °C for 15 min and kept constant for the entire printing process. HEPA filter was activated setting 100% air flow, ensuring the sterility of the working area during the entire printing process and finally UV light was turned off. There is no treatment after printing for scaffolds which were 3D printed with the pellets that have undergone the described process. For the non-sterile printing, the process to be followed is the same except for the fact that before printing the material is heated directly to 90 °C for 30 min and both the UV light and the HEPA filter were switched off.

Bioprinter set-up

Before starting printing, INKREDIBLE+ needs to be homed and calibrated. The 3D printer set-up involves three steps: a) XYZ homing axes to position the printhead in the middle of the print-bed; b) Z axis calibration to tune properly the

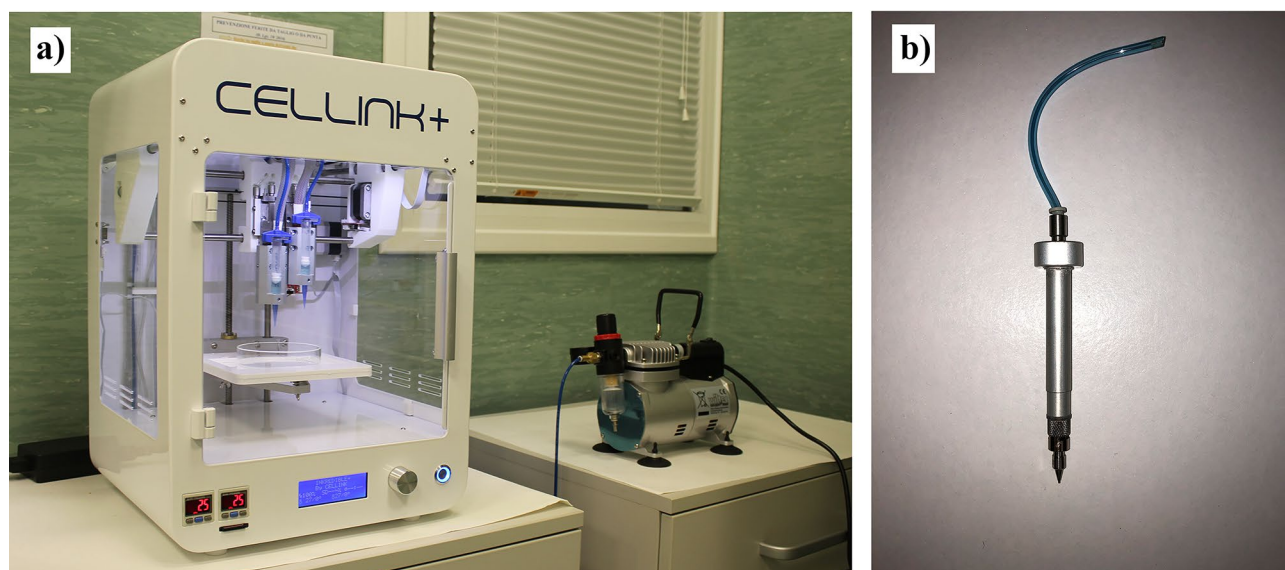


Fig. 3 a) Cellink INKREDIBLE+ pneumatic extrusion-based 3D bioprinter. b) Aluminum cartridge connected to a 0.5 mm metal nozzle used for extruding 90%PCL-10%HA at temperatures above 50 °C

distance between the nozzle and the printing bed, which is crucial for the first layer printing; c) the pressure calibration, to find the optimal pressure value that enables a proper flow of material. In this case, 150 kPa was the optimal pressure to guarantee a constant composite extrusion.

Scaffold design and 3D printing

Using Solidworks® software (Dassault Systèmes SolidWorks Corporation, United States) we created an 8 mm of diameter and 0.7 mm of height cylindrical structure. Then, the 3D virtual model was sliced using Slic3r, a free slicing software. During the slicing process, we defined some parameters such as layer height, perimeter, printing speed, infill percentage, and so on. The infill percentage is an important parameter for 3D printing as it determines the distance between two adjacent filaments, hence, it defines the pore size of the scaffold. The relevant pore size ensures proper cell adhesion, proliferation, differentiation, and scaffold colonization. After the slicing we obtained a structure made of two 0.35 mm of height layers with one perimeter. The printing speed was set at 45 mm min⁻¹ that associated with a 150 kPa pressure allowed constant extrusion of 90%PCL-10%HA composite and its correct adhesion on the Petri dish. The specific set of instructions, that is to say the G-code, was created and scaffolds were 3D printed. We printed scaffold using both the 90%PCL-10%HA composite which underwent the sterilisation process described in Sect. 2.3.2 and the composite which did not undergo it.

Thermal characterization of 3D printed scaffolds

We investigated the thermal properties of 3D printed scaffolds to verify whether the high temperature, due to the sterilisation process, could influence its thermoplastic property. We created a CAD model using the process described in Sect. 2.3.4 setting 40% infill percentages. We performed DSC and Simultaneous Thermogravimetric Analysis (TGA/DSC) supported by ATR Fourier transform infrared (FTIR) spectroscopy. We performed analysis on i) pellets, ii) 3D printed scaffolds using 90%PCL-10%HA pellets sterilised following the process described in Sect. 2.3.2, and iii) pellets which did not undergo it. Moreover, we performed an analysis on 3D printed scaffolds with 100% PCL pellets to evaluate whether the thermoplastic properties of the material were influenced by HA inclusion. Measurements were carried out at least in triplicate.

Differential scanning calorimetry

DSC analyses were performed with a Mettler STAR[®] system (Mettler Toledo, Milan, Italy) equipped with a DSC821[°] Module and an Intracooler device for the sub-ambient

temperature analysis (Julabo FT 900) on 3–4 mg (Mettler M3 Microbalance) samples in sealed aluminum pans with pierced lid in a range temperature from 0 to 200 °C (heating rate $b = 10 \text{ K min}^{-1}$). All the experiments were conducted in a nitrogen atmosphere (flux rate 50 mL min⁻¹) in order to prevent oxidative degradation. The instrument was previously calibrated with Indium as standard reference.

Simultaneous thermogravimetric analysis

The mass losses were recorded with a Mettler STAR[®] system (Mettler Toledo, Milan, Italy) TGA with simultaneous DSC (TGA/DSC1) on 3–4 mg samples in alumina crucibles with lid, in a range temperature from 30 to 500 °C (heating rate $b = 20 \text{ K min}^{-1}$). All the experiments were conducted in a nitrogen atmosphere (flux rate 50 mL min⁻¹) in order to prevent oxidative degradation. The instrument was previously calibrated with Indium as standard reference.

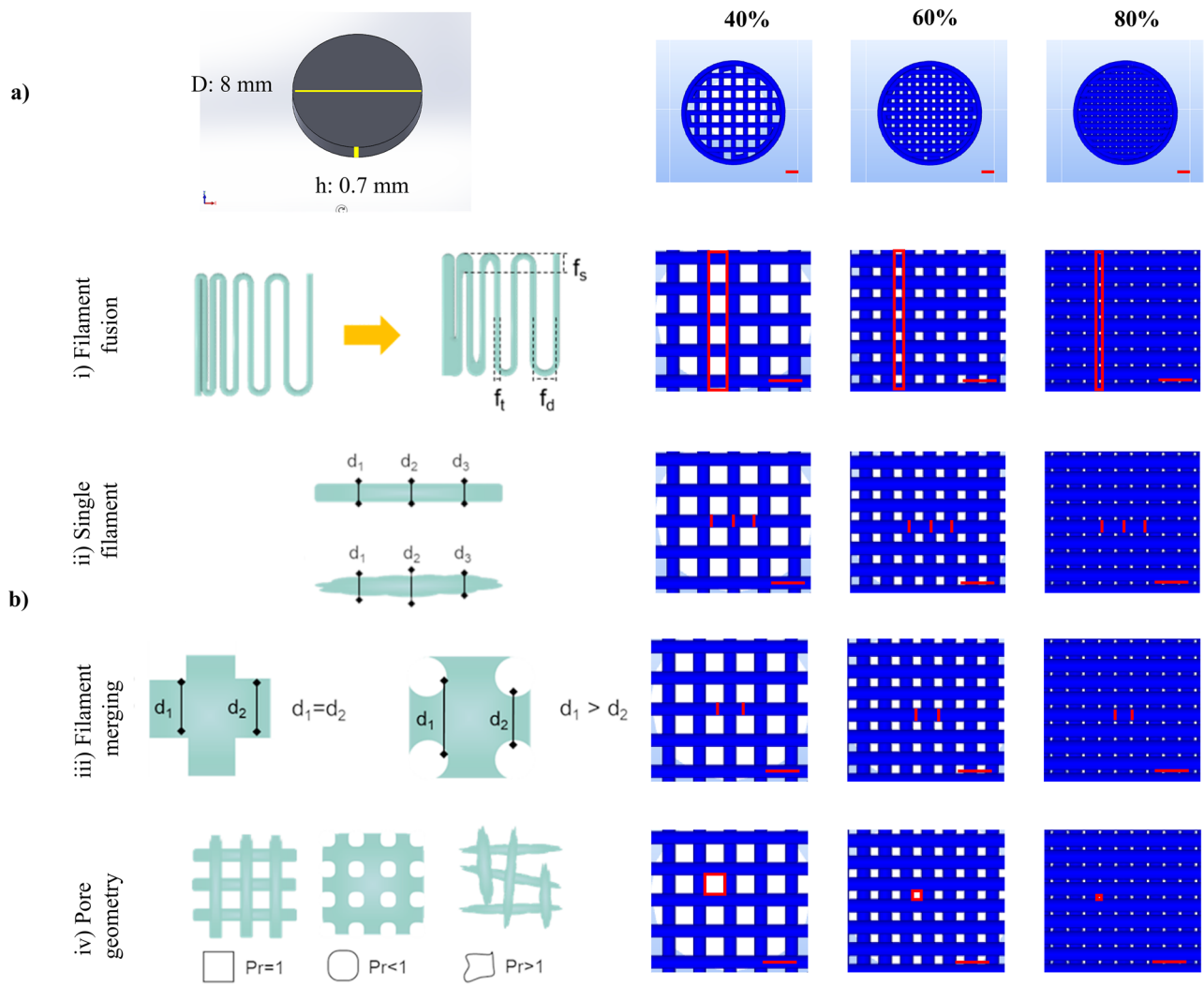
ATR Fourier transform infrared spectroscopy

The IR spectra were recorded using a Fourier transform infrared spectrophotometer (Perkin Elmer Spectrum One, Monza, Italy) with a single reflection ATR accessory (PIKE MIRacle™). The samples as such were placed on the ATR crystal of ZnSe and pressed on the crystal. The spectra were collected in transmittance mode within the spectral range of 650–4000 cm⁻¹ with 64 scans and a resolution of 4 cm⁻¹.

Assessment of printing performance

In order to assess the printing performance, we created the CAD virtual model using the process described in Sect. 2.3.4 considering three different infill percentages: 40%, 60%, and 80% (Fig. 4a). We evaluated the printability, including the analysis of extrudability, shape fidelity, and filament characterization of the 3D printed scaffold using extrusion-based 3D printer following the protocol implemented by Schwab et al. [27] (Fig. 4b). Moreover, we evaluated the impact of the sterilisation process on printing performance. The protocol consists in performing four quantitative tests described as follows.

- A. *Filament fusion*: adjacent filaments, deposited in a meandering pattern at increasing filament distances (fd), can merge due to the surface tension between the material and the collector substrate, as well as between each layer of a material (Fig. 4b.i).
- B. *Filament uniformity*: single filaments are evaluated on their homogeneity based on the filament diameter (d1, d2, and d3), with identical diameters characterizing a homogeneous filament (Fig. 4b.ii).



		3D virtual model target dimension		
Test	Parameters (mm)	40% infill	60% infill	80% infill
A - Filament fusion	Filament distance	0.493	0.179	0.02
B - Filament uniformity	Filament diameter	0.45	0.45	0.45
C - Filament merging	Filament diameter $d_1=d_2$	0.45	0.45	0.45
D - Pore geometry	Printability index	1	1	1

Fig. 4 Assessment of printing performance. **a)** 3D virtual model with a cylindrical structure of 8 mm of diameter and 0.7 mm of height was sliced increasing infill percentages: 40%, 60%, and 80%. **b)** Assessment of printability and shape fidelity, including the analysis

of extrudability, shape fidelity, and filament characterization of 3D printed scaffold using extrusion-based 3D printer following method proposed by Schwab and colleagues [27], scale bar 1 mm. **c)** 3D virtual model target dimensions. Adapted from [27]

- C. *Filament merging*: analysis of filament diameter and merging with focus on the intersection/overlay of two filaments (Fig. 4b.iii).
- D. *Pore geometry*: analysis of transversal pore geometry with optimal rectangular pore shape for ideal filament (Fig. 4b.iv) using printability index (P_r) [28] calculating as:

$$P_r = \frac{p^2}{16a}$$

where p and a are pore perimeter and area, respectively.

We set up the 3D printer according to the steps described in Sect. 2.3.3. We 3D printed twelve scaffolds (four for each infill considered) using the 90%PCL-10%HA composite that underwent the sterilisation process described in Sect. 2.3.2 and four with the composite which did not undergo it (total of 24 samples). 3D printed constructs were analysed using a stereomicroscope (Olympus Sz61, Olympus Corporation, Japan) with a digital camera (Infinity1, Teledyne Volumera, Canada). Scaffold's images were acquired, and ImageJ software (National Institutes of Health, United States) was used to extract the parameters required by protocol, i.e., filament distance, filament diameter, and printing index. The standard deviations were calculated to assess scaffold printing repeatability.

3D virtual model vs. 3D printed model

The parameters of the 3D virtual model were extracted and considered as targets (Fig. 4c). To compare 3D virtual model and printed scaffold we calculated printing error as the difference between 3D virtual and 3D printed model. GraphPad Prism (GraphPad Software, United State) was used to perform two-way ANOVA to evaluate statistically significant differences between virtual model and printed scaffolds with and without a sterilisation process to evaluate the impact of the sterilisation process on printing performance.

Protocol for the evaluation of the sterilisation process

To assess sterility of the printed scaffolds we followed the protocol described by USP [26] which involves the immersion of the scaffolds into a soybean-casein digest medium (SCDM or TBS) for 14 days. SCDM was selected for its ability to support the growth of a wide range of aerobic bacteria and fungi (i.e., yeasts and molds). We first created the CAD model using the process described in Sect. 2.3.4, then we set 40% as infill percentages during the slicing process. We 3D printed six scaffolds using 90%PCL-10%HA pellets sterilised following the process described in Sect. 2.3.2 and other six scaffolds which did not undergo it.

Sterility test evaluation was carried out under aseptic conditions, in fact all the equipment and medium were previously sterilised by autoclave, and the pH of sterilised medium was evaluated in order to respect 7.1 – 7.5 after the sterilisation process as described by USP. The protocol to validate scaffolds sterility involves the following steps: i) sterile tubes were filled with 2 ml of SCDM; ii) printed scaffolds (one per tube) were immersed into SCDM and tubes were closed; iii) two tubes filled only with SCDM (no scaffolds inside) and used as control; iv) tubes were incubated for 14 days at 25–27 °C and at 37 °C (Fig. 5); iv) every two days scaffolds were monitored to evaluate any evidence of microorganism growth. To avoid contamination, no other samples were inside the incubator. Growth was assessed by the presence of turbidity 1, 7 and 14 days and, at its conclusion, we examined the medium for macroscopic evidences of microbial growth. The test was performed in triplicate.

To further confirm the effectiveness of the proposed sterilisation methods we performed quantitative tests of microbial growth inhibition through colony counting technique.

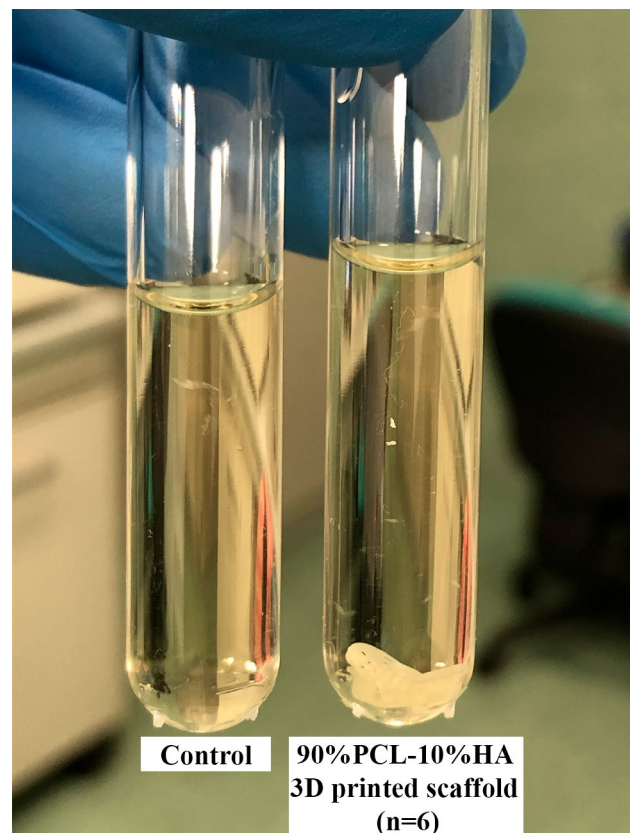


Fig. 5 Scaffold sterility evaluation protocol: scaffolds printed with sterilised ($n=6$) and no-sterilised ($n=6$) 90%PCL-10%HA pellets were immersed into 2 ml of SCDM and incubated for 14 days both at 20–25 and 37 °C. Moreover, two tubes were filled only with medium as control. Every two days, the SCDM of scaffolds was monitored for evaluating any evidence of turbidity due to microorganism growth

After the incubation time, four scaffolds printed with pellets sterilised following the process described in Sect. 2.3.2 and four scaffolds not treated with the proposed protocol were tested for the validation of the liquid test into SCDM–Agar for colony counting.

Results and discussion

90%PCL-10%HA composite fabrication

We successfully produced 90%PCL-10%HA pellets using a laboratory scale Co-rotating Twin Screw Extruder. During the compounding activity, we produced 10 gr of pellets based on composite PCL + 10%wt HA with dimensions compliant to cartridges. The proposed technique allows the fabrication of composite materials pellets to be used with the adopted extrusion-based 3D printing technology. Furthermore, according to Kim and colleagues [5], we are able to modulate the HA percentages according to the application of interest (e.g., bone and cartilage TE). We decided to investigate only one percentage of HA (10% wt.) to define the process which represents the main object of the proposed work. In future works, other HA percentages will be investigated as well as biological tests.

3D bioprinter set-up

We successfully set-up a commercial 3D extrusion based bioprinter to print 90%PCL-10%HA composite pellets produced with a Co-rotating Twin Screw Extruder. Although extrusion temperature of the composite during pellets production had been 60–65 °C, printing temperature was set at 90 °C because it is the temperature that allows to extrude the proposed 90%PCL-10%HA composite using the Cel-link INKREDIBLE + bioprinter. Compared to a screw system based-bioprinter, it needs higher temperature to extrude the material and to achieve constant extrusion. Pressure and printing speed were fixed at 150 kPa and 45 mm min⁻¹ respectively following the previous preliminary calibration test. These are the optimal values that allow 90%PCL-10%HA composite constant extrusion as well as filament adhesion on the Petri dish. We did not perform targeted study on the extrusion strand thickness because it is out of scope, although it is important for the printing process workflow.

Thermal characterization of 3D printed sterilised scaffolds.

The DSC profile of 100% PCL pellet is characterized by an endothermic effect with a maximum peak temperature at $T_{\text{melt}} = 63.7 \pm 0.4$ °C, due to melting ($DH_{\text{melt}} = 72 \pm 7$ J g⁻¹)

which is followed by sample decomposition (Fig. 6a, curve i). The anhydrous nature of 100% PLC is confirmed by the thermogravimetric analysis (Fig. 6b, curve i) that does not reveal any weight loss until about 300 °C, temperature at which decomposition of the melt begins. In detail, under nitrogen fluxes the TGA curve of 100% PCL pellet shows a one-step degradation, due to a single weight loss of $97 \pm 2\%$, corresponding to polymer pyrolysis. The initiation of degradation occurs at $T_{\text{onset}} = 344.3 \pm 0.5$ °C and the final temperature is at $T_{\text{endset}} = 461.8 \pm 0.2$ °C with a maximum decomposition peak at $T_{\text{max}} = 423.1 \pm 0.3$ °C (T_{max} calculated by the first order derivative of the TGA curve). The temperature and enthalpy parameters for scaffolds printed with not sterilised and sterilised 100% PCL pellets (Fig. 6a, curves ii and iii respectively) are not statistically different, showing that the process does not modify the crystallinity of the polymer [29, 30]. Moreover, the degradation of the polymer is not influenced by the preparation method, in fact the TGA curves of the scaffolds printed with not sterilised and sterilised pellets are superimposable (Fig. 6b, curves ii and iii respectively). The thermal analysis is supported and confirmed by FT-IR spectroscopy. The 100% PCL pellets spectra, scaffolds printed with not sterilised and sterilised 100% PCL pellets are shown and compared with each other in Fig. 6d (curves i, ii and iii respectively). In all the spectra the characteristic bands of the 100% PCL can easily be identified, such as at 2924 e 2851 cm⁻¹ the asymmetric and symmetric CH₂ stretching, at 1721 cm⁻¹ the carbonyl stretching, at 1293 cm⁻¹ the C-O and C-C stretching characteristic of the crystalline phase and at 1163 cm⁻¹ the symmetric COC stretching. The difference absence of relative intensity and position of the bands confirm the lack of influence of the preparative method on 100% PCL.

The DSC curves of scaffold 3D printed with not sterilised and sterilised 90%PCL-10% HA pellets are reported in Fig. 6d. The presence of HA determines a shift to lower temperature and enthalpy values of the PLC melting peak in the treated samples. In particular, the DSC curve of 90%PCL-10%HA pellet is typical of an anhydrous sample with an endothermic effect due to the melting ($T_{\text{melt}} = 64.4 \pm 0.3$ °C; $DH_{\text{melt}} = 65 \pm 6$ J g⁻¹). In the printed scaffolds the temperature peaks are registered at $T_{\text{melt}} = 58.7 \pm 0.4$ °C and $T_{\text{melt}} = 61.1 \pm 0.8$ °C for the not sterilised and sterilised, respectively. The enthalpy is reduced by about 20% indicating a slight loss in the crystallinity following printing probably due to the presence of HA in the mixture. On the other hand, the HA inclusion does not influence the stability of the products, in fact TGA curves did not show significant variations in the onset and endset temperatures of the degradation process (curve not reported). The FT-IR spectra registered on the same scaffolds containing HA were not highlight significant differences in position and intensity of the PCL characteristic bands (spectra not reported). The thermal data

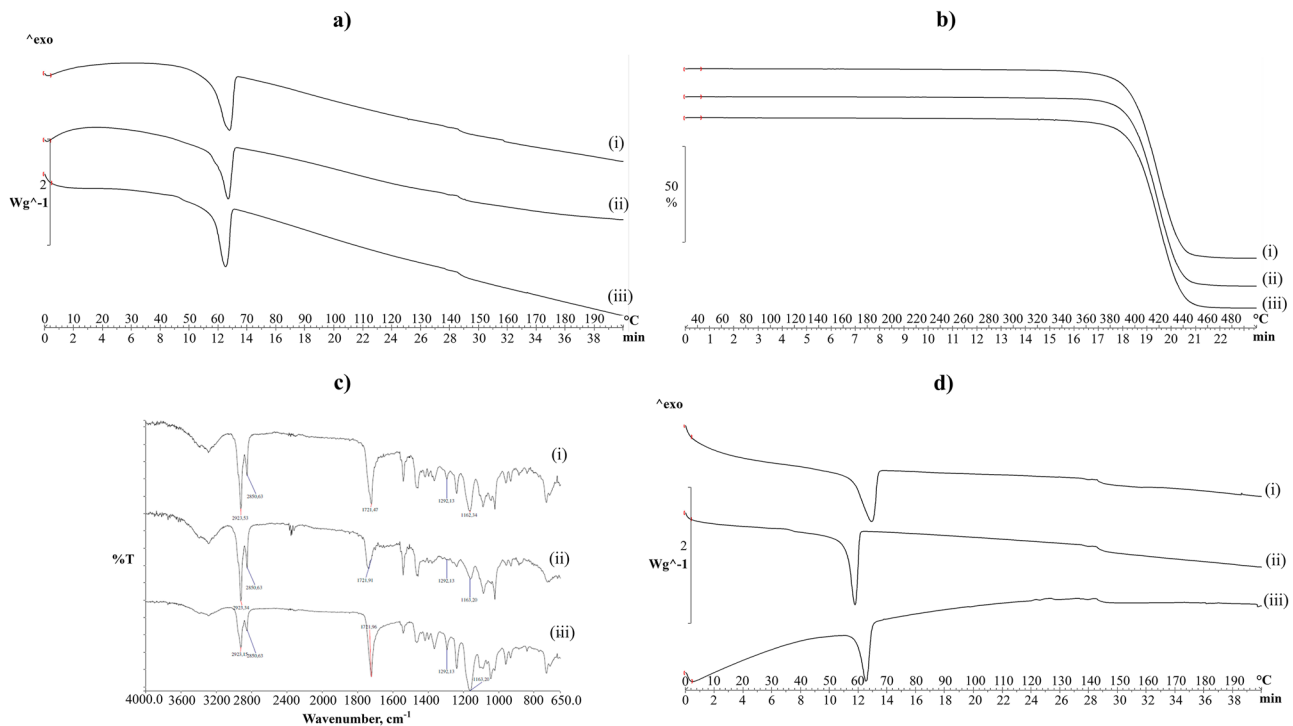


Fig. 6 Results of thermal analysis of 100% PCL and 90%PCL-10%HA composite. **a)** DSC curves, **b)** TGA curves, and **c)** FT-IR spectra of 100% PCL (i) pellet as such, scaffold 3D printed with (ii)

not sterilised, and (iii) sterilised with PCL pellets. **d)** DSC curves of 90%PCL-10%HA (i) pellet as such, scaffolds 3D printed with (ii) not sterilised, and (iii) sterilised PCL-HA pellets

supported by FT-IR confirmed that printed and sterilisation processes did not significantly influence the crystallinity and stability of material both with and without HA.

Assessment of printing performance

We 3D printed 90%PCL-10%HA sterilised and not sterilised composite pellets using a pneumatic extrusion-based 3D bioprinter although 60% is the maximum infill that can be used to discriminate pores (Fig. 7a), so we did not take into account 80% infill for next analysis. The results of quantitative tests to assess the fidelity of sterilised and not sterilised 90%PCL-10%HA 3D printed composite are summarized in Fig. 7b and 7c. In test A, we evaluated filament fusion calculating the filament distance of 3D printed scaffolds for 40% and 60% infill. The filament distance ranged between 0.184 ± 0.03 mm and 0.472 ± 0.008 mm. Results according to literature: it is generally considered that the strain distance between 100 and 500 μ m is beneficial for cell proliferation, migration and nutrient transport for bone TE [31]. Filament diameters were calculated to assess both filament uniformity (test B) and merging (test C). Filament diameter is higher for scaffolds 3D printed with sterilised 90%PCL-10%HA composite. Filament uniformity is ensured with a standard deviation < 0.03 mm, while there are no differences between d_1 and d_2 for test C, so the filament overlap is constant and

repeatable. Pore geometry was assessed in test D calculating P_r that is about 1. The result means that scaffolds pores have optimal rectangular pore shape for all analysed cases.

Figure 8 shows the impact of the sterilisation process of 3D printed scaffolds. There are significant differences ($*p < 0.002$) between scaffolds printed with sterilised and not sterilised 90%PCL-10%HA composite considering filament distance and diameter (Fig. 8a and b). Considering the printing index, there are not significant differences between sterilised and not sterilised 90%PCL-10%HA composite (Fig. 8c).

Comparing the 3D virtual model to the 3D printed one, there are significant differences between 3D model and scaffolds 3D printed with sterilised composite for 40% infill and non-sterilised composite for 60% infill. Results are evident also considering printing error both for 40% and 60% infill (data summarized in Table 1). Printing error decreases by increasing infill in both the scaffolds printed with the material which either underwent the sterilisation process or did not. In addition, we observed that the printing error is greater for scaffolds printed with the sterilised composite for 40% infill scaffolds, while it is lower than for the non-sterilised one. We assume that the difference due to the preheating of the composite in the cartridge during the sterilisation process which causes a greater dissolution of material and presumably a decrease in viscosity. This causes a greater collapse

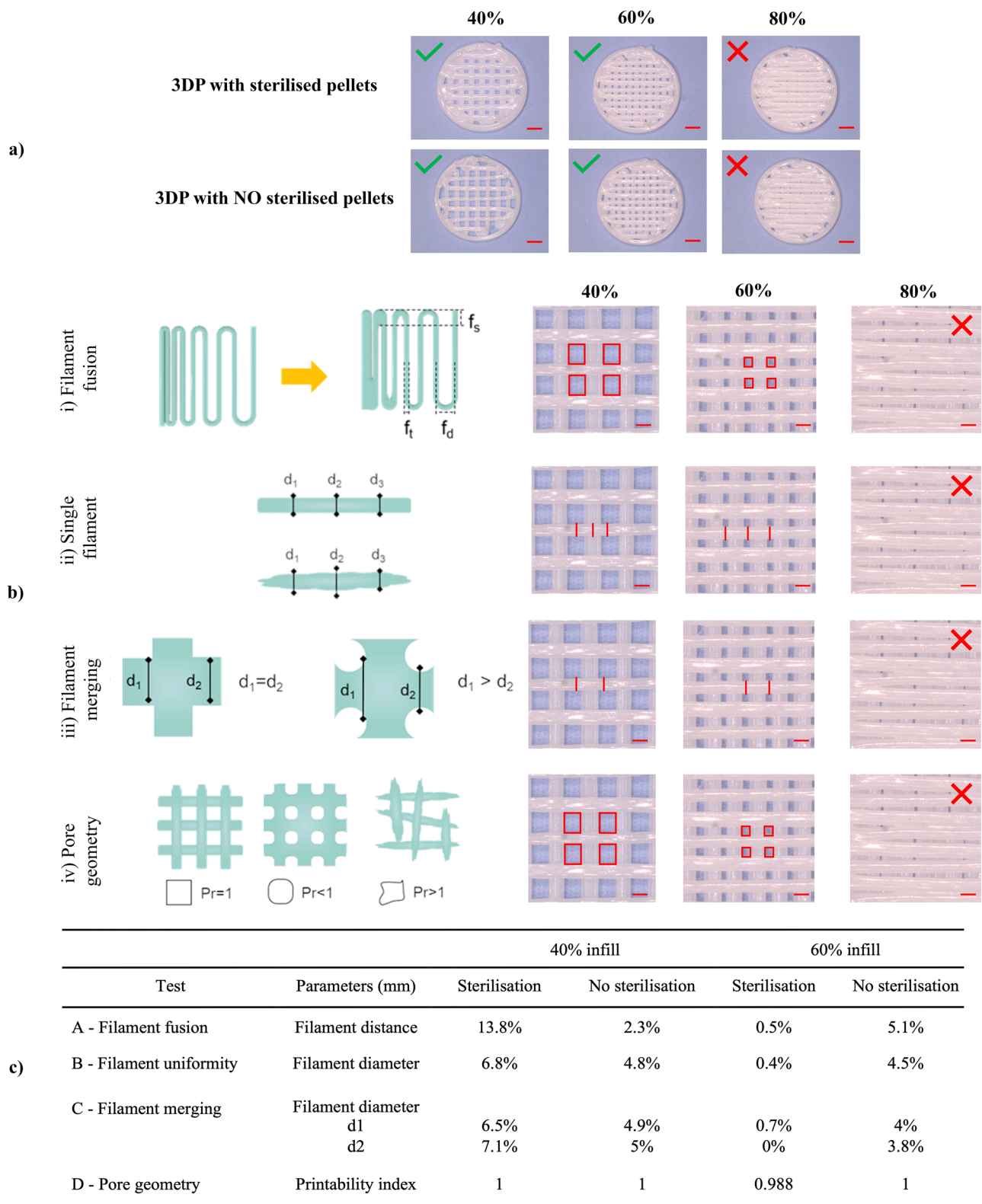
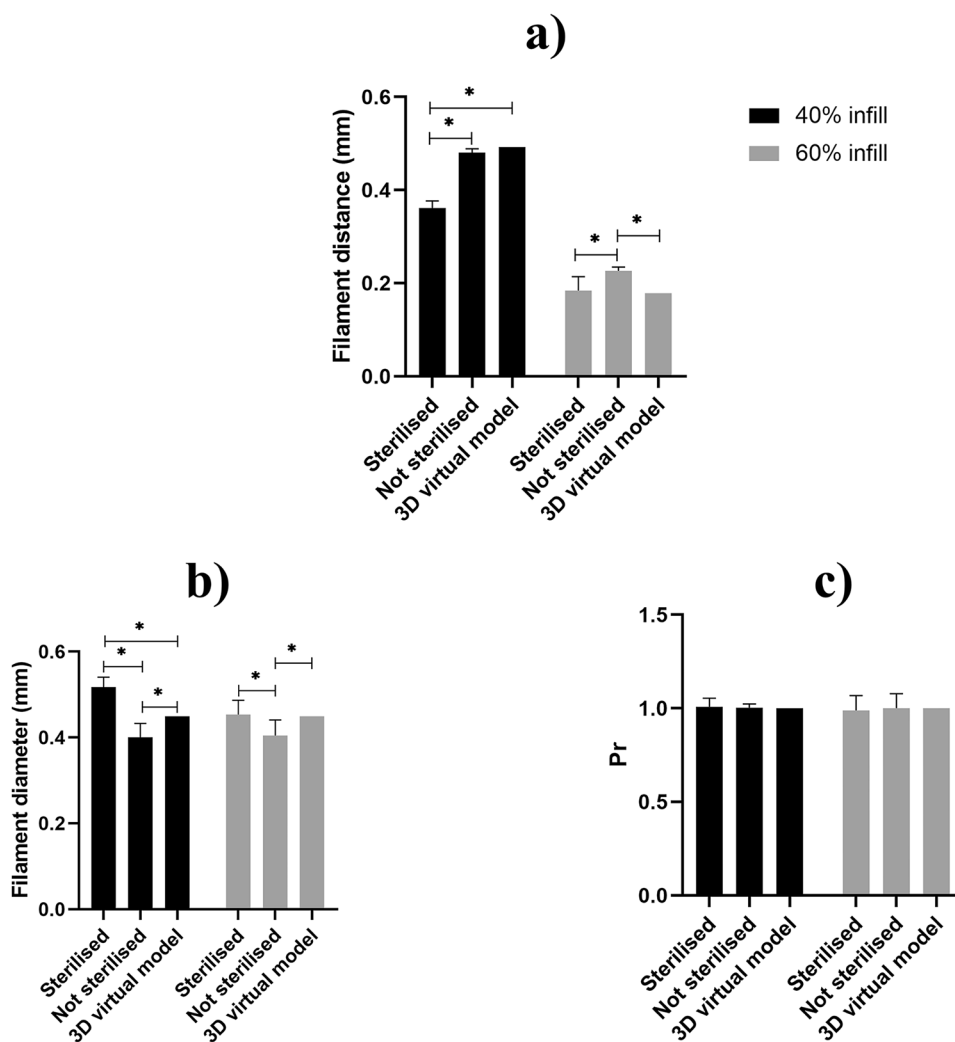


Fig. 7 3D printed scaffold with and without sterilisation process. **a)** 60% is the maximum infill that can be used to discriminate pores, so scaffolds with 80% infill were not taken into account for next analysis. **b)** Results of quantitative tests for assessing fidelity of sterilised

and not sterilised 90%PCL-10%HA 3D printed composite. **c)** Mean and standard deviation of scaffold geometrical parameters 3D printed with sterilised and not sterilised 90%PCL-10%HA composite. *Scale bar 1 mm*

Fig. 8 3D virtual model was compared with the 3D printed one. Two ways ANOVA was performed for evaluating statistically significant differences between samples 3D printed with sterilised and not sterilised pellets (P-value: *p < 0.002)



of the structure during the printing process, so the scaffolds that have undergone the sterilisation process deviate more from target values compared to the structures printed with the material that has not undergone the sterilisation process. This issue is not limited to the scaffold production, since the lower viscosity of the material can be compensated by a proportional reduction of printing pressure, through testing. The opposite effect occurs in the case of 60% infill scaffold in which printing error is lower for scaffolds printed with the sterilised composite.

Protocol for the evaluation of the sterilisation process

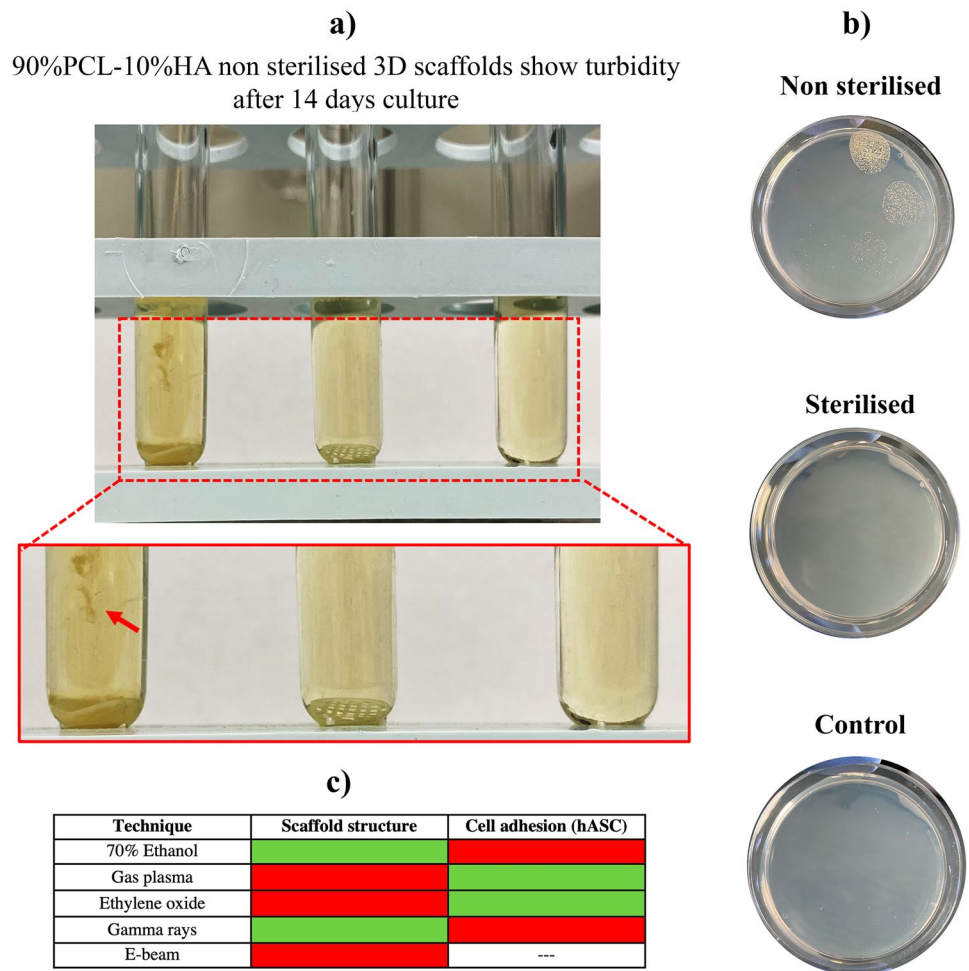
There are different methods to verify a component sterility according to the type of the product to be tested; according to Bugno et al. [23], we followed the protocol described by USP [26] which foresees the immersion of the scaffolds into SCDM for 14 days and incubated at 26 °C and 37 °C.

The medium in which the scaffolds printed with 90%PCL-10%HA pellets that did not undergo the sterilisation process

Table 1 Printing error calculated as difference between 3D virtual and 3D printed model

Test	Parameters (mm)	Sterilisation	No sterilisation	Sterilisation	No sterilisation
A - Filament fusion	Filament distance	13.80%	2.30%	0.50%	5.10%
B - Filament uniformity	Filament diameter	6.80%	4.80%	0.40%	4.50%
C - Filament merging	Filament diameter				
	d1	6.50%	4.90%	0.70%	4%
	d2	7.10%	5%	0%	3.80%
D - Pore geometry	Printability index	0.80%	0.30%	1.20%	0%

Fig. 9 **a)** On day 14, the SCDM does not show turbidity for both the control samples and the scaffolds printed with the pellet that underwent the proposed sterilisation process; on the other hand, the medium in which the scaffolds printed without the sterilisation process were immersed, shows both turbidity and the presence of microorganism's growth (highlighted by the red arrow). **b)** Quantitative proofs of microbial growth inhibition through colony counting technique showed the presence of microorganism's growth for scaffolds printed with non-sterilised pellet. **c)** Different traditional sterilisation techniques we performed before reaching proposed process. Green indicated successful and orange indicates non successful. None of them were suitable both in terms of integrity of the scaffold structure and cell adhesion with human Adipose Stem Cells (hASC)



described in Sect. 2.3.2 where immersed, showed turbidity already after one and a half day of culture highlighting a growth of microorganisms (Fig. 9a). After 14 days, three out of six non-sterile scaffolds showed turbidity due to aerobic microbial growth. Meanwhile, the medium containing scaffolds printed with 90%PCL-10%HA pellets that underwent to proposed process did not show turbidity throughout the incubation period, so no evidence of aerobic microbial growth was found. The quantitative proofs of microbial growth inhibition through colony counting technique showed the presence of microorganism's growth for scaffolds printed with non-sterilised pellet (Fig. 9b), confirming the effectiveness of the proposed sterilisation methods.

In this case, the inactivation of microorganisms is due to the high temperatures, as the process in autoclave modality, while the UV light allows to ensure sterility of the printing area [32].

The assessed protocol for the pellet sterilisation, which consist in heating the material at 120 °C for 30 min before printing is effective, enables us to print the composite in sterile conditions allowing us to obtain a sterile printed product ready to be used for 3D in vitro cell culture without any

treatment after printing. Before reaching this process, we performed different sterilisation techniques that are generally used in literature [24] but none of them were suitable both in terms of integrity of the scaffold structure and cell adhesion with human Adipose Stem Cells (Fig. 9c).

As a future development of the present work, we propose to analyse whether the temperature and duration of the treatment can affect sterilisation.

Conclusion

We 3D printed a 90%PCL-10%HA sterile composite using a pneumatic extrusion-based bioprinter and we set up a framework able to assess the printing performance and the sterility degree of the 3D printed scaffolds. The use of the 3D printer according to the proposed protocol allows us to obtain sterile finished scaffolds ready to be seeded with cells and used for TE applications. Furthermore, the methodology used to sterilise PCL-HA pellets does not affect thermal properties. The proposed methodology has the advantage to be simple to be applied without the need of specific instrumentation

beside the 3D printer and a UV source, if not already available inside the bioprinter and it can be easily extended to other thermo-plastic materials employed in TE field.

Acknowledgements The authors acknowledge the project “3D-printed bioscaffolds for bone transplant—Progetto di Ricerca Corrente 2018” of IRCCS Policlinico San Matteo of Pavia (Italy).

Funding Open access funding provided by Università degli Studi di Pavia within the CRUI-CARE Agreement.

Declarations

Conflicts of interest The authors declare that there is no conflict of interest.

Open Access This article is licensed under a Creative Commons Attribution 4.0 International License, which permits use, sharing, adaptation, distribution and reproduction in any medium or format, as long as you give appropriate credit to the original author(s) and the source, provide a link to the Creative Commons licence, and indicate if changes were made. The images or other third party material in this article are included in the article’s Creative Commons licence, unless indicated otherwise in a credit line to the material. If material is not included in the article’s Creative Commons licence and your intended use is not permitted by statutory regulation or exceeds the permitted use, you will need to obtain permission directly from the copyright holder. To view a copy of this licence, visit <http://creativecommons.org/licenses/by/4.0/>.

References

- Hutmacher DW (2000) *Biomaterials* 21(24): 2529–2543
- Fan D, Stauffer U, Accardo A (2019) *Bioengineering* 6(4):113
- Zhang H, Mao X, Du Z, Jiang W, Han X, Zhao D, Han D, Li Q (2016) *Sci Technol Adv Mater* 17(1):136–148
- Kim MH, Yun C, Chalisserry EP, Lee YW, Kang HW, Park SH, Jung WK, Oh J, Nam SY (2018) *Mater Lett* 220:112–115
- Kim JW, Shin KH, Koh YH, Hah MJ, Moon J, Kim HE (2017) *Materials* 10(10):1123
- Tian L, Zhang Z, Tian B, Zhang X, Wang N (2020) *RSC Adv* 10(8):4805–4816
- Itälä A, Ylänen HO, Yrjans J, Heino T, Hentunen T, Hupa M, Aro H (2002) *T. J Biomed Mater Res* 62(3):404–411
- Shim JH, Huh JB, Park JY, Jeon YC, Kang SS, Kim JY, Rhie JW, Cho DW (2013) *Tissue Eng. Part A* 19(3–4):317–328
- Bastianini M, Scatto M, Sisani M, Scopece P, Patelli A, Petracchi AJ (2018) *Compos Sci* 2(2):31
- Lee JY, Cho B, Wu B, Lee M (2013) *Biofabrication* 5(4):045003
- Chuenjitkuntaworn B, Inrung W, Damrongsri D, Mekaapiruk K, Supaphol P, Pavasant PJ (2010) *Biomed. Mater Res, Part A* 94(1):241–251
- Ke D, Yi H, Est-Witte S, George S, Kengla C, Lee SJ, Atala A, Murphy SV (2019) *Biofabrication* 12(1):015022
- Aljohani W, Ullah MW, Zhang X, Yang G (2018) *Int J Biol Macromol* 107:261–275
- Gungor-Ozkerim PS, Inci I, Zhang YS, Khademhosseini A, Dokmeci MR (2018) *Biomater Sci* 6(5):915–946
- Kačarević ŽP, Rider PM, Alkildani S, Retnasingh S, Smeets R, Jung O, Zrinka I, Barbeck M (2018) *Materials* 11(11):2199
- Jiao Z, Luo B, Xiang, S, Ma H, Yu, Y, Yang W (2019) *Adv Industrial Eng Polym Res* 2(4):196–202
- Trachtenberg JE, Placone JK, Smith BT, Fisher JP, Mikos AG (2017) *J Biomater Sci Polym Ed.* 28(6):532–554
- Gerdes S, Mostafavi A, Ramesh S, Memic A, Rivero IV, Rao P (2020) *Tamayol A. Tissue Eng, Part A* 26(5–6):279–291
- Park SA, Lee SH, Kim WD (2011) *Bioprocess Biosyst. Eng* 34(4):505–513
- Montanari L, Costantini M, Signoretti EC, Valvo L, Santucci M, Bartolomei M, Fattibene P, Onori S, Faucitano A, Conti B, Genta I (1998) *J. Controlled Release* 56(1–3): 219–229
- Baume A, Coleman N, Boughton PJ (2009) *Biomimetics Biomater. Tissue Eng* 4:59–69
- Griffin M., Naderi N, Kalaskar DM, Malins E, Becer R, Thornton CA, Whitaker IS, Mosahebi A, Butler PEM, Seifalian AM (2018) *Int J Biomater*
- Bugno A, Saes DPS, Almodovar AAB, Dua K, Awasthi R, Ghisleni DDM, Hirota MT, De Olivera WA (2018) *Pinto, T. D J A J Pharm Innovation* 13(1):27–35
- Dai Z, Ronholm J, Tian Y, Sethi B, Cao XJ (2016) *Tissue Eng* 7:2041731416648810
- MMTO, Gopalakrishnan V, Samsuddin AR, Al Salih KA, Shamsuria O (2007) *Archives of Orofacial Scien* 2(1):41–44
- United States Pharmacopeia- USP 40/NF 35 <1223> (2017) Validation of alternative microbiological methods, The United States Pharmacopeia Convention, Rockville, MD, United States
- Schwab A et al (2020) "Printability and Shape Fidelity of Bioinks in 3D Bioprinting." *Chem Rev*
- Ouyang L, Yao R, Zhao Y, Sun W (2016) Effect of bioink properties on printability and cell viability for 3D bioplotting of embryonic stem cells. *Biofabrication* 8:035020
- Coiai S, Scatto M, Conzatti L, Azzurri F, Andreotti L, Salmini E, Stagnaro P Zanolin S, Cicogna F, Passaglia E (2011) *Polym Adv Technol* 22(12):2285–2294
- Vega JF, Fernández-Alcázar J, López JV, Michell RM Pérez-Camargo RA, Ruell B, Martínez-Salazar J, Arnal ML Dubois P, Müller AJ (2017) *J Polym Sci Part B: Polym Phys* 55(17):1310–1325
- Hollister SJ (2005) *Nat Mater* 4 (7):518e524
- Mori M, Hamamoto A, Takahashi A, Nakano M, Wakikawa N, Tachibana S, Ikehara T, Nakaya Y, Akutagawa Y, Kinouchi Y (2007) *Med Biol Eng Comput* 45(12):1237–1241

Publisher’s Note Springer Nature remains neutral with regard to jurisdictional claims in published maps and institutional affiliations.